Fatigue-Resistant Nylon Alloys

M. G. WYZGOSKI* and G. E. NOVAK

Polymers Department, General Motors Research and Development Center, Warren, Michigan 48090

SYNOPSIS

Crystalline nylon 66 was modified by blending with both an amorphous nylon and a rubber-modified amorphous nylon. The ternary blends exhibit a 50–100-fold decrease in fatigue crack propagation rates, even at rubber concentrations of only 1 or 2%. These same blends do not necessarily exhibit improved impact strength and the examination of a variety of alloys and blends demonstrates that fatigue and impact fracture mechanisms are distinctly different. The fracture surface morphologies indicate that the basic fatigue fracture mechanism of craze coalescence for nylon 66 is not changed by alloying. However, the presence of the rubbery phase leads to cavitation and ductile drawing that retard the craze breakdown and coalescence processes without evidence of crack tip blunting. Surprisingly, the addition of rubber-modified nylon 66 to a nylon 66 matrix does not impart as great an improvement in fatigue resistance as does the miscible amorphous nylon. Also, alloys having improved impact strength are observed to exhibit inferior fatigue resistance. These results demonstrate that the excellent fatigue resistance of crystalline polymers can be improved even further by judicious selection of alloying ingredients optimized specifically for fatigue fracture.

INTRODUCTION

The ever-expanding usage of polymeric materials in semistructural applications has resulted in a need to better understand the fatigue fracture behavior of these materials. Though extensive literature on fatigue failure mechanisms exists, it is also apparent that the measurement and/or prediction of the fatigue resistance of a given polymer presents a formidable task. For example, even though numerous reports have been published on the fatigue properties of unmodified nylon 66, there was considerable confusion in the literature concerning the influence of test frequency.[1-3] A previous report has described the difficulties in assessing the fatigue behavior of unfilled nylons and has clearly demonstrated the role of cyclic loading frequency.[4] Other reports have described the influence of glass fiber orientation on fatigue fracture for both injection- and reaction-molded nylons.[5,6] In the case of the more recently introduced polymer blends and alloys, there exists even less data on fatigue behavior. Generally, these engineering plastics were formulated to meet requirements such as dimensional stability, processability, or high impact strength rather than being optimized for fatigue resistance. A correlation between fatigue strength and impact strength might be expected; however, this study will show that this is not true. Supertough alloys can exhibit inferior fatigue behavior and, conversely, a nominally brittle material can show excellent fatigue properties. With this in mind, the present study was undertaken to investigate material modifications that would lead to improvements in the fatigue resistance of nylon 66. The intent was to achieve this goal without largely impairing the excellent thermal and chemical resistance of the nylon by restricting the addition of alloying agents to relatively low concentrations (less than 10% by weight).

EXPERIMENTAL

Materials

The nylon 66 employed in this study was Zytel 122L, which was provided by the E. I. duPont Company.

* To whom correspondence should be addressed.

Journal of Applied Polymer Science, Vol. 51, 873–885 (1994)
 CCC 0021-8995/94/050873-13

Alloying agents were selected from commercially available polymers that were known to be compatible with nylon 66.[7] This included an amorphous nylon, Trogamid T, manufactured by Dynamit Nobel, and a rubber-toughened amorphous nylon, Bexloy AP C-803 (originally designated 8203Q), from DuPont. In addition, a reactive ethylene propylene diene monomer (EPDM) rubber, Uniroyal X465, was investigated along with an acrylic core-shell rubber modifier, 8586B, from the Rohm and Haas Co. A nylon 66-based alloy, Noryl GTX 900, from the General Electric Co. was also examined.

Processing

Polymer blends were prepared by melt processing using a Werner and Pfleiderer ZSK-30 twin-screw extruder with the processing conditions given in Table I. The binary blends were prepared by a single extrusion of the dry-blended pellets. The ternary blends were prepared in a two-step process. First, the reactive rubber modifiers were initially melt-blended with the amorphous nylon and, subsequently, pellets of this toughened system were dry-blended with nylon 66 and extruded a second time. A control sample of the pure nylon 66 was also extruded and pelletized in order to take into account the added thermal history of the extrusion step. Also, in some cases, the rubber modifiers were added directly to the nylon 66 matrix to assess the role of the rubber alone.

All materials were dried both before and after extruding into pellet form for subsequent injection molding into end-gated plaques that were 50.8 by 203.2 by 3.2 mm. Standard molding conditions for the preparation of nylon 66 plaques were employed for all the blends. Following molding, the plaques were stored in desiccators to maintain their dry-as-molded state and all testing was performed using only dry samples.

Table I Processing Conditions for Extrusion Blending

Temperature zone 1	249–255°C
Temperature zone 2	274–280°C
Temperature zone 3	275–280°C
Temperature zone 4	276–286°C
Temperature zone 5	270–275°C
Melt temperature	283–285°C
Torque	84–99%
Pressure	0.48–0.62 MPa
Screw speed	300 rpm
Throughput	130–150 g/min

Fatigue Testing

Fatigue crack propagation measurements were performed using compact tension specimens whose geometry is identical to that previously described.[6] All samples were cut from the center of the plaques. Gate or end effects were not specifically investigated. Precracks were cut parallel to the melt flow to minimize any influence of orientation on crack growth rates. Fatigue tests were conducted at a frequency of 0.5 Hz under load control. Measurements of the crack propagation rates were made from the video-recorded images as described in earlier studies.[5,6] A thermography camera was used to monitor the sample temperature and to ensure that hysteretic heating did not occur at the fatigue crack tip during the test.[4]

Mechanical Properties

The flexural moduli of the various samples were determined by cutting strips, 12.7 mm wide and oriented along the flow direction, from the plaques and flexing them at 5 mm/min in an Instron Model 1125. The Izod impact strength was also assessed for notched test strips following ASTM D 256. However, the latter were cut transverse to melt flow to cause fracture in the same direction as in the fatigue experiments.

Fracture Surface Morphology

An ISI Model DS-130 scanning electron microscope was used to examine the fracture surface that was produced by stable fatigue crack propagation. The fatigue fracture surface was examined from the initial razor cut precrack up to the point where unstable fast fracture had occurred.

RESULTS

Fatigue Crack Propagation Rates

Measurement Precision

Although fatigue resistance can be rapidly assessed by measuring crack growth rates using the fracture mechanics approach previously described,[4–6] it must be recognized that significant scatter can occur in this type of measurement. For the injection-molded nylons, the reproducibility of the test is excellent within a given batch of molded test plaques.[4] However, more significant scatter occurs when comparing results of several different molding trials, particu-

larly over a long time period. Figure 1 shows a summary plot of fatigue crack propagation measurements made for dry as-molded nylon 66. The data represent measurements made at a frequency of 0.5 Hz, which minimizes any contribution of hysteretic heating.[4] It is not known whether the different plots reflect real differences in the test plaques (such as molecular weight, orientation, or crystallinity) or simply are due to the measurement precision. For the purpose of this report, the important point is that sizable changes in fatigue crack growth rates must be observed before one has confidence that material differences exist. The results in Figure 1 also indicate that less scatter occurs at lower ΔK levels, where da/dN values differ by a factor of 2.5, compared to a factor of 10 at higher ΔK levels. In the following figures, the unmodified nylon 66 is represented by the data labeled A in Figure 1. This particular sample was extruded and repelletized to provide a similar thermal history to that experienced by the twin-screw extruded blends.

Fatigue-resistant Blends

Based upon early fracture surface morphology studies, it was hypothesized that improvements in the toughness of the amorphous phase of the semicrystalline nylon 66 would provide improved fatigue resistance. Thus, blends of amorphous nylon and crystalline nylon were investigated. The fatigue properties of the individual components were evaluated first and these results are shown in Figure 2. The data for the unmodified amorphous nylon clearly indicate that this material is inferior to nylon 66 in resistance to fatigue crack propagation. This is not surprising in view of the known advantage of crystalline materials in this regard.[1] What is surprising is the result for the toughened amorphous nylon showing that it too exhibits poorer fatigue resistance than that of the pure nylon 66 despite its far superior impact strength. This is a clear indication that fatigue and impact fracture mechanisms are distinct and that toughening and alloying systems may not necessarily be optimized for both failure modes. Other examples will be discussed in a later section. For the purposes of the present discussion, it is important to recognize that blending of either amorphous nylon or toughened amorphous nylon would not be predicted to improve the fatigue crack propagation resistance of the nylon 66 based upon the results in Figure 2.

Initial blends were prepared by adding only 10% of the amorphous nylons to the crystalline nylon 66. This was in keeping with an additional goal of attempting to modify fatigue properties without producing radical changes in modulus, thermal stability, or chemical resistance. Fatigue crack propagation

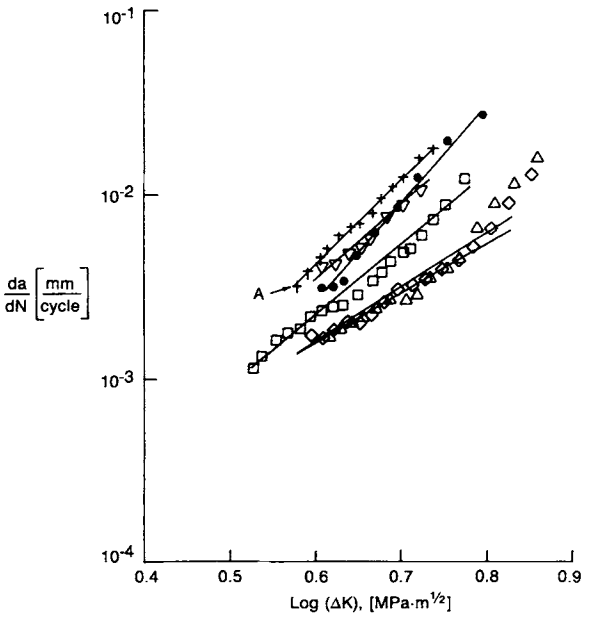

Figure 1 Batch-to-batch variability in fatigue crack propagation rates for unmodified nylon 66. Data labeled A are for a reextruded control sample for comparison with blends.

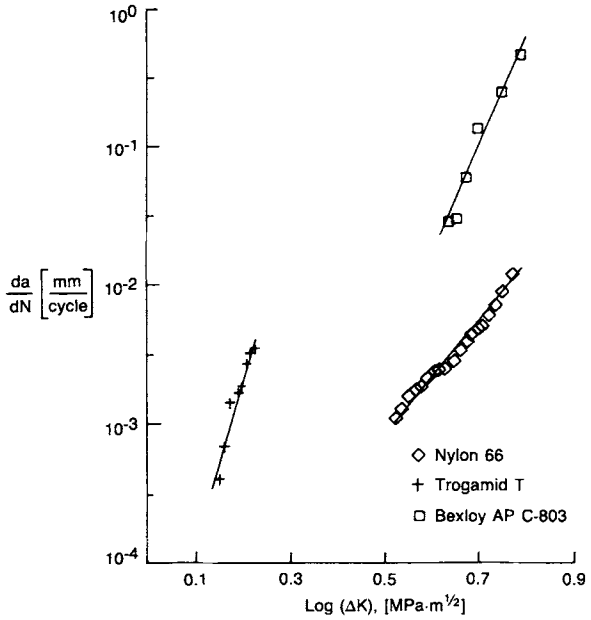

Figure 2 Comparison of fatigue crack propagation rates for an amorphous nylon (Trogamid T), a rubber-toughened amorphous nylon (Bexloy AP C-803), and crystalline nylon 66.

rates for these blends are shown in Figure 3. There is a marginal improvement (lower crack growth rates at a given ΔK level) for the alloy containing an amorphous nylon (Trogamid T); however, the blend containing the toughened amorphous nylon (Bexloy AP C-803) shows a much more significant decrease in fatigue crack growth rates. Even the addition of only 5% of this material resulted in a significant improvement, as shown in Figure 4. The blend containing 15% did not exhibit a much greater effect and higher levels were not investigated.

The different results for the two amorphous nylons shown in Figure 2 were suspected to be due to the presence of the rubber-toughening agent in the Bexloy material rather than to differences in chemical structure between the Bexloy and the Trogamid T. This was investigated further by preparing rubber-modified versions of the Trogamid T using a reactive EPDM from Uniroyal (X465). Figure 5 shows a comparison of the fatigue behavior of nylon 66 blends containing either the Bexloy material or the 80/20 Trogamid T/X465 preblend. These results demonstrate the significant role of the rubber phase in achieving the greatly improved resistance to fatigue crack growth. In fact, the preblend using the Trogamid T amorphous nylon is seen to be even more effective than using the toughened Bexloy resin.

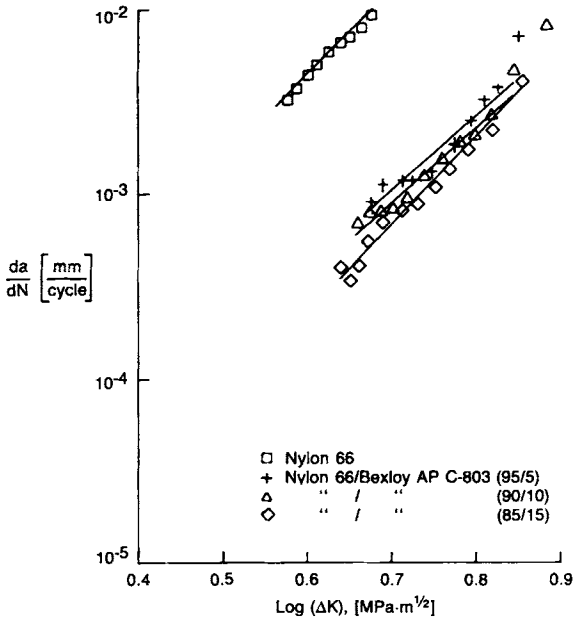

Figure 4 Effect of concentration of Bexloy AP C-803 on fatigue crack propagation rates of nylon 66 blends.

The direct addition of the reactive rubber to the nylon 66 was also investigated. As shown in Figure 6, the rubber alone is effective in reducing fatigue crack growth rates; however, it is not as effective as

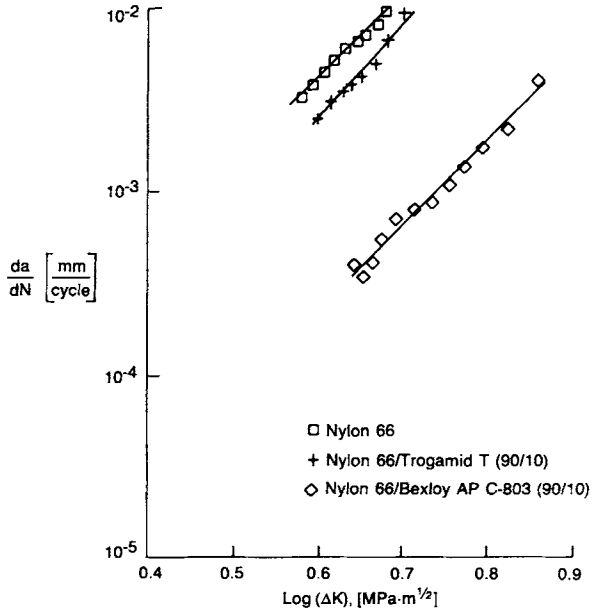

Figure 3 Fatigue crack propagation rates for nylon 66 and blends with 10% of either Trogamid T or Bexloy AP C-803.

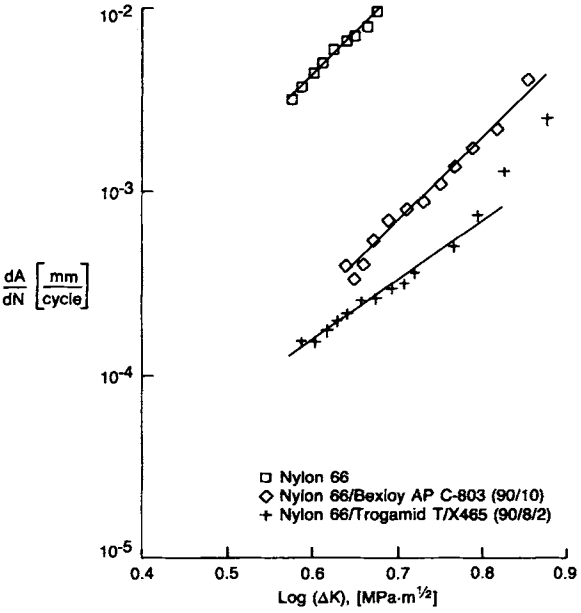

Figure 5 Comparison of fatigue crack propagation rates for nylon 66 blends with either 10% Bexloy AP C-803 or 10% of an 80/20 Trogamid T/X465 preblend.

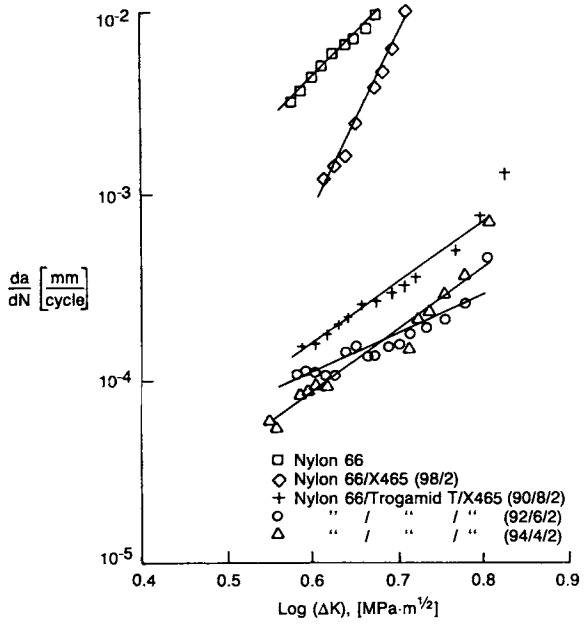

Figure 6 Fatigue crack propagation rates for nylon 66 containing 2% of X465 reactive rubber modifier added with and without the amorphous nylon, Trogamid T, in varying ratios.

the alloys containing amorphous nylon also. These results suggest that the miscible amorphous nylon does play a key role in imparting improved fatigue resistance to the crystalline nylon 66. At a rubber concentration of 4%, the fatigue crack propagation rates were still reduced to a greater extent by the ternary blend, as shown in Figure 7. In this case, the advantage of the ternary blend over the binary blend is less than that observed at only 2% rubber (Fig. 6). The use of higher ratios of amorphous nylon to rubber did not provide significantly different results, nor did the addition of 10% of preblends having amorphous nylon/rubber ratios of 6/4, 5/5, or 4/6. All these systems exhibited excellent fatigue resistance with crack propagation rates that were generally 50–100 times lower than that observed for the unmodified nylon 66.

In addition to the use of the reactive EPDM rubber, an evaluation was also made of a butyl acrylate-based acrylic elastomer having a core/shell structure. This reactive rubber modifier was reported to be effective as an impact modifier for nylon 6 but not for nylon 66. By first preparing a preblend of the modifier with amorphous nylon, it was found that the fatigue behavior of nylon 66 was, in fact, greatly improved with this elastomer. Results are shown in Figure 8. Thus, it appears that, in general, any rubber-modified amorphous nylon can be expected to be an effective alloying agent to improve the fatigue resistance of nylon 66. Subsequent studies using the acrylic rubber indicated that it was more sensitive to processing variables than was the EPDM material and further work was discontinued.

The previous results have demonstrated that very small amounts of a rubber-toughening agent can be extremely effective in retarding the growth of a fatigue crack in a nominally brittle polymer matrix. Though the role of the rigid glassy amorphous nylon polymer is not clear, a possible explanation is that it acts to more uniformly disperse the rubber phase at these relatively low concentrations. Assuming that its efficiency is a consequence of the fact that it is completely miscible with the nylon 66, it could be predicted that similar dispersion efficiency would be possible by using a rubber-modified nylon 66 as the alloying or dispersing agent. Obviously, the nylon 66 with a grafted rubber modifier would be completely soluble in the unmodified nylon 66 matrix. This type of ternary blend was evaluated using a commercially available supertough nylon 66 (Zytel 801) that contained 20% of an EPDM rubber. The fatigue crack propagation behavior of these blends is shown in Figure 9. Measurable improvements are noted for the blends containing 10 or 20% of toughened nylon 66. Interestingly, these blends are not

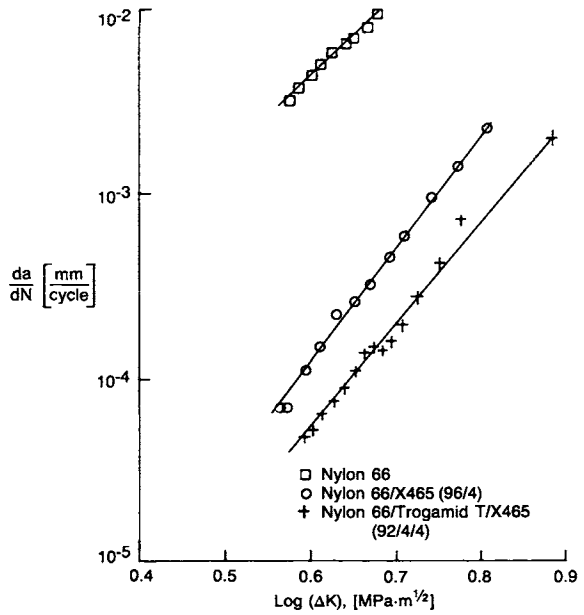

Figure 7 Effect of adding 4% X465 reactive rubber to nylon 66 with and without the amorphous nylon, Trogamid T.

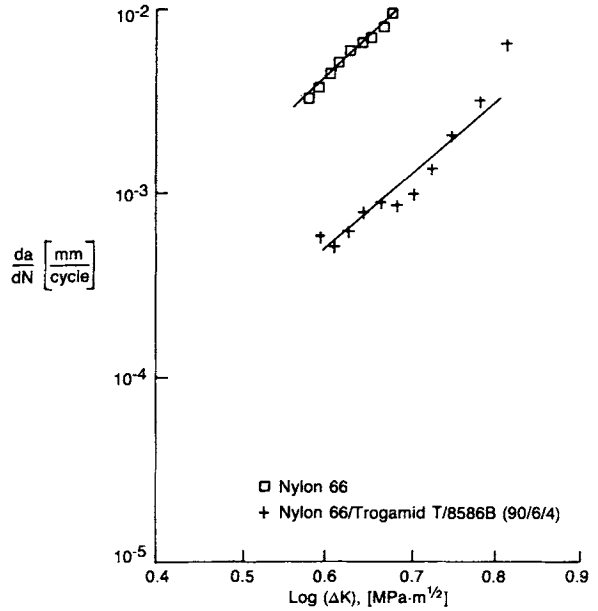

Figure 8 Fatigue crack propagation rates for nylon 66 blended with amorphous nylon and a core-shell rubber modifier, 8586B.

as efficient as equivalent blends in which the same amount of rubber is grafted onto the amorphous nylon (dashed lines in Fig. 9). The reason for the difference is not known at this time; however, the available data suggest that the amorphous nylon is the preferred polymer for the preblend.

Figure 10 shows fatigue crack growth rate data for the pure Zytel 801 supertough nylon 66. This material is highly resistant to fatigue crack initiation, and stable fatigue crack propagation could only be produced at very high ΔK levels. In fact, at the ΔK levels employed for the supertough nylon, most nylons would have fractured immediately since the maximum stress intensity level in the fatigue experiment would have exceeded the fracture toughness of the materials. A comparison of the supertough nylon 66 with the ternary blend system containing only 4% rubber is also shown in Figure 10. The data are difficult to compare due to the differing slopes. At low ΔK, no crack growth was measurable for the supertough material. This suggests that further increases in rubber concentration above 4% would most likely not lead to reduced crack propagation rates, but would, instead, shift the region of stable crack growth to higher ΔK levels similar to the supertough material. These results also demonstrate that the use of only 4% rubber in the blend is very effective in inhibiting fatigue crack growth at high ΔK levels even though much higher rubber concentrations (15–20%) are needed for impact strength improvement.

Throughout the course of this study, it has become evident that alloys or blends that exhibit in-

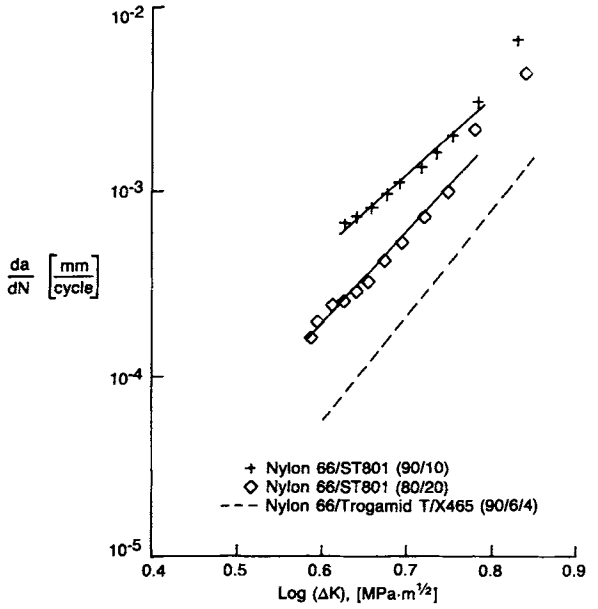

Figure 9 Fatigue crack propagation rates for nylon 66 blended with rubber-toughened nylon 66. Dashed lines represent a comparable blend using rubber-toughened Trogamid T.

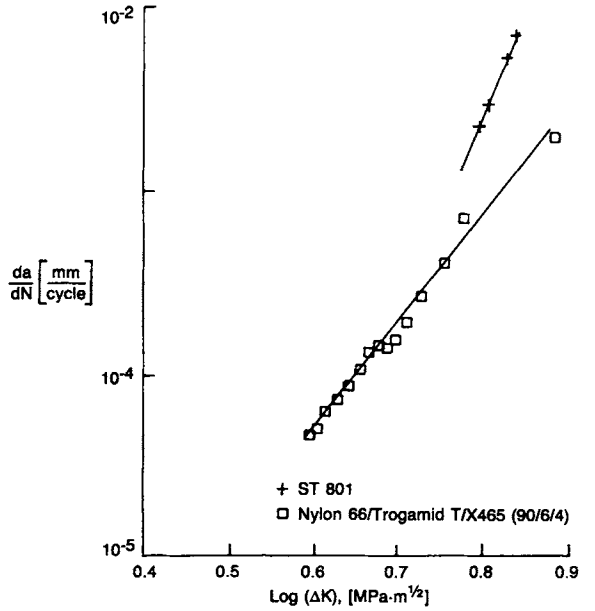

Figure 10 Fatigue crack propagation rates for a laboratory-prepared ternary blend and a commercial supertough nylon 66 (Zytel ST 801).

creased toughness may not necessarily show improved fatigue resistance. An additional example of this behavior was observed while examining the propagation of fatigue cracks in Noryl GTX, a nylon 66-based alloy. This material is a complex mixture of a rubber-toughened immiscible amorphous poly(phenylene oxide) phase that is dispersed in a crystalline nylon 66 matrix. A polymeric compatibilizer is also added to the blend. Not only is it well established that this material has improved impact strength compared to nylon 66, but the toughening mechanism has also been extensively described in the literature and used as a model system.[8,9] Figure 11 shows a comparison of the fatigue crack propagation rates for Noryl GTX and nylon 66. These data were taken at a frequency of 5 Hz rather than at the usually employed rate of 0.5 Hz. The Noryl GTX exhibits significantly increased crack growth rates at all ΔK levels, indicating that it is inferior to the unmodified nylon in spite of its toughness under impact-loading conditions. It was of interest to apply the nylon-blending technology of the present study to possibly improve the fatigue resistance of the Noryl GTX. The results given in Figure 11 demonstrate that the blending of GTX with the rubber-toughened amorphous nylon does, in fact, reduce the fatigue crack growth rates, making the material more comparable to nylon 66, especially at the lower ΔK levels. Further improvements would be expected with the addition of higher concentrations of the EPDM rubber. Of course, the success in improving the GTX material suggests that the blend technology may be applicable to any nylon-based material system.

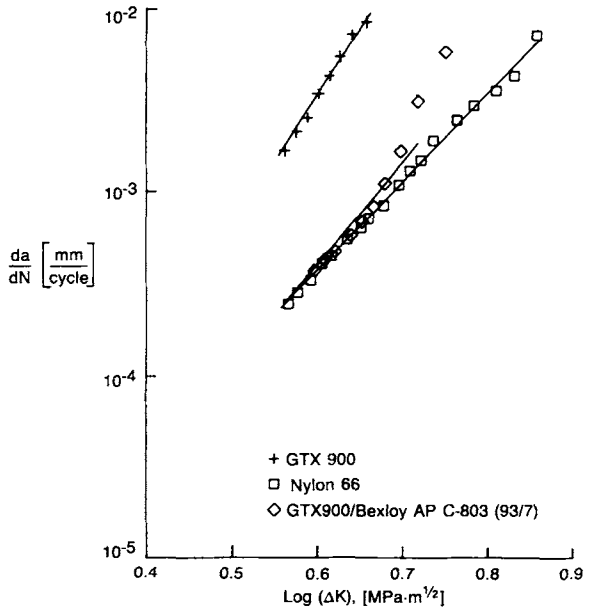

Figure 11 Fatigue crack propagation rates for nylon 66, Noryl GTX 900, and an alloy using Noryl GTX 900 as the base resin.

Initiation of Fatigue Cracks

The ASTM E-647 procedure for measurement of fatigue crack propagation rates recommends that the initial extension of the precrack be ignored in data collection.[10] In other words, it is anticipated that some transient effects may exist initially before the stable fatigue crack is propagating in a well-behaved manner. Although the ASTM procedure is generally followed in this and previous studies of nylon fatigue fracture, no unusual behavior had been noted for the initiation of fatigue cracks from the razor-cut precracks in the unmodified nylons. In the present study of nylon blends, however, it was observed that the initial crack growth data did not always follow the same Paris equation plot as did the subsequent stable phase of crack propagation. In all cases, the initial crack growth rates were higher than expected but decreased rapidly or remained constant at higher ΔK values as the fatigue crack continued to grow. A typical example of this is shown in Figure 12(a), where it can be seen that the crack growth rate appears to decelerate at the lowest ΔK levels before an acceleration begins, which is the more typical or expected behavior (i.e., follows the Paris equation). In an extreme case, the initial period of anomalous crack growth, which appears to be independent of the magnitude of the stress intensity level, is extended over a broad range of ΔK levels as shown in Figure 12(b). Another example is shown in Figure 13(a), where it is noted that the dependence of the crack growth rate on ΔK is very slight throughout most of the test. The anomalous behavior of the blends was not observed in all cases and was difficult to reproduce in any specific blend. These examples are provided to demonstrate that the behavior of the nylon blends can be different from the more straightforward fatigue crack propagation in the unmodified nylon 66.

The above results suggested that the growth of the fatigue crack from the razor cut precrack was more accelerated than was the corresponding growth from the natural fatigue crack. This was confirmed in experiments where the fatigue crack was allowed to propagate and then the stress intensity level was reduced (by decreasing the load) to near the initiation value at the start of a test. As shown in Figure 13(b), the measured crack growth rates from this

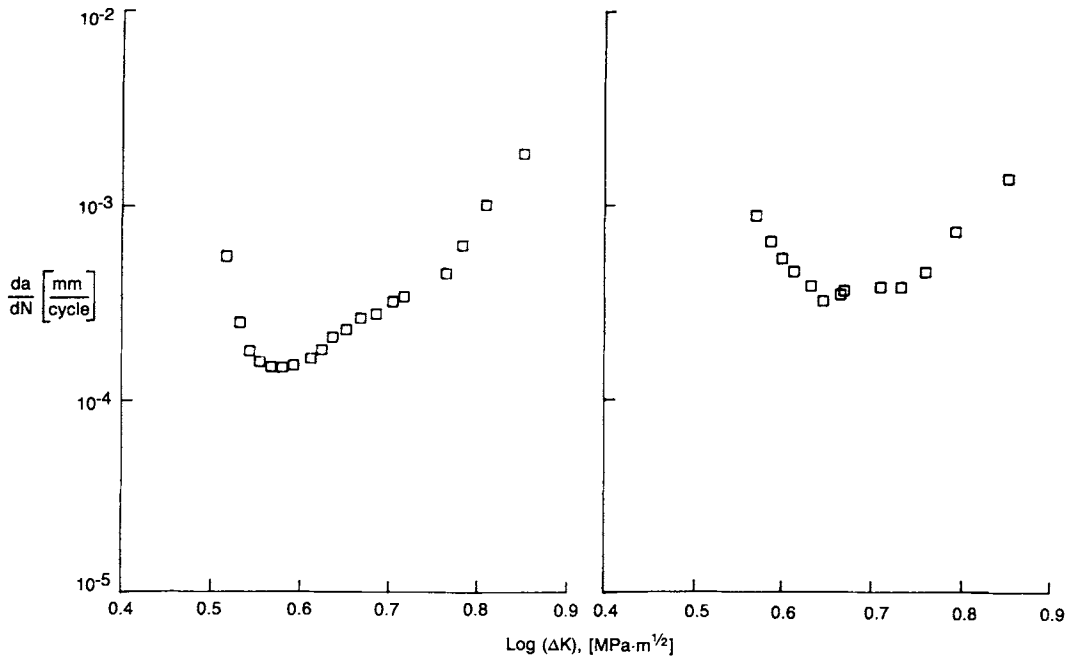

Figure 12 Fatigue crack propagation rates for nylon 66 blends showing anomalous crack growth rates at low stress intensity levels: (a) 90/8/2-nylon 66/Trogamid T/X465; (b) 90/10-nylon 66/Bexloy AP C-803.

fatigue precrack were found to decrease to values that fit on the Paris plot for the particular blend. This implies that the relative or local stress intensity at the razor cut was, in fact, higher than that at a natural or fatigue crack in the same material. This is tentatively attributed to the development of a

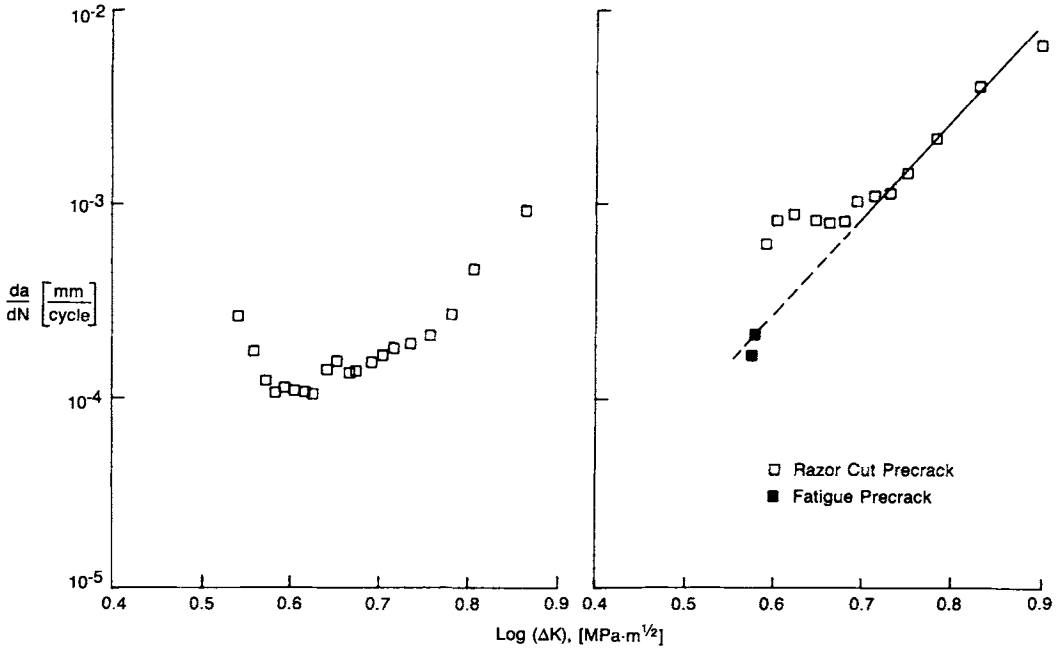

Figure 13 Further examples of anomalous fatigue crack propagation behavior in nylon 66 blends: (a) 92/6/2-nylon 66/Trogamid T/X465; (b) 95/5-nylon 66/Bexloy AP C-803, also showing data measured from a fatigue precrack (solid points).

unique damage or deformation zone at the fatigue crack tip, as has been observed by others.[11] An optical microscopy study of the crack tip damage zone is underway to confirm this hypothesis for the nylon blends by comparing the results to the unmodified nylon 66.[12]

Mechanical Properties

The flexural moduli and Izod impact strengths of several nylon alloys are given in Table II. For comparison, the values for unmodified nylon 66 and a supertough material are also listed. These results clearly show that neither the impact strength nor the stiffness of the blended nylons are significantly changed. In view of the dramatic improvements in fatigue fracture resistance for the blends, it is apparent that a straightforward correlation does not exist between impact and fatigue fracture. These results also demonstrate that the fatigue-resistant blends retain the excellent stiffness of the nylon 66 matrix. In contrast, a significant loss of modulus is noted for the supertough nylon 66.

Fracture Surface Morphology

The patchy-type fracture surface that is characteristic of fatigue failure in dry nylon materials has been described extensively in previous reports and is shown again here in Figure 14.[4,5] The fatigue-resistant blends also exhibit a patchy-type structure (Fig. 15), and at low magnifications, the fracture surface of the alloys is indistinguishable from that of the pure nylon 66. However, at higher magnifications, the blends exhibit a porous, foamy appearance that is not seen in the unmodified nylon 66. This is shown in Figure 16. The large voids are suspected to be caused by the cavitation and deformation of the rubber particles.

The blends could also be distinguished from the pure nylon because their fracture surfaces did not exhibit a uniform texture from the crack initiation region to the final fast fracture at the end of the fatigue test. Specifically, the fracture surface underwent a transition from the modified patchy structure to a smoother and more homogeneous microcracking pattern as shown in Figure 17.

The microcracking is similar in appearance to classical fatigue striations as the pattern is oriented

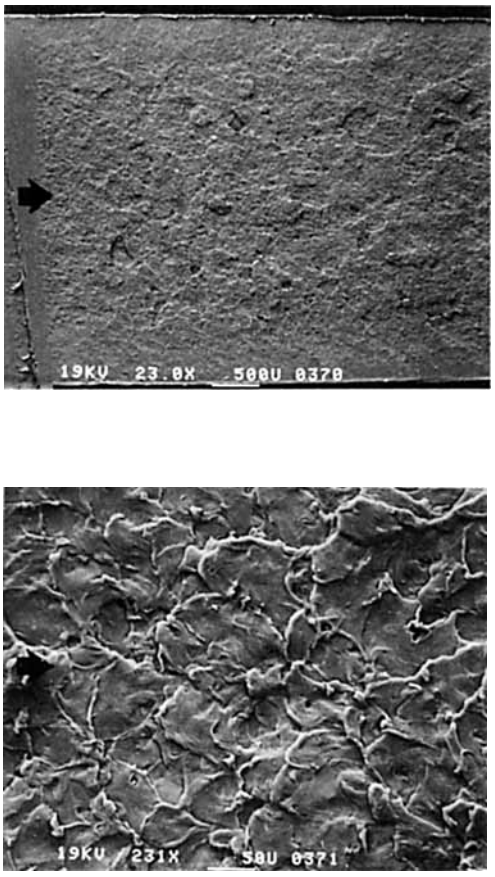

Figure 14 Scanning electron microscopy of the fatigue fracture surface for unmodified nylon 66 showing patchy-type regions at magnifications of (a) 23× and (b) 230×. Arrows indicate crack growth direction in this and subsequent figures.

Table II Mechanical Properties of Nylon 66 and Blends with Rubber-modified Amorphous Nylon

Composition (%)			Flexural Modulus (GPa)	Izod Impact (J/m)
Nylon 66	Amorphous Nylon	Rubber		
100	0	0	2.9	20
90	10	0	2.9	17
95	4[a]	1[a]	2.9	22
90	8[a]	2[a]	2.8	26
85	12[a]	3[a]	—	31
80[b]	0	20	1.7	783
94	4[c]	2[d]	2.8	67
92	6[c]	2[d]	2.9	75
92	4[c]	4[d]	2.8	108
90	5[c]	5[d]	—	99

[a] Bexloy AP C-803.
[b] Zytel ST801.
[c] Trogamid T.
[d] X465.

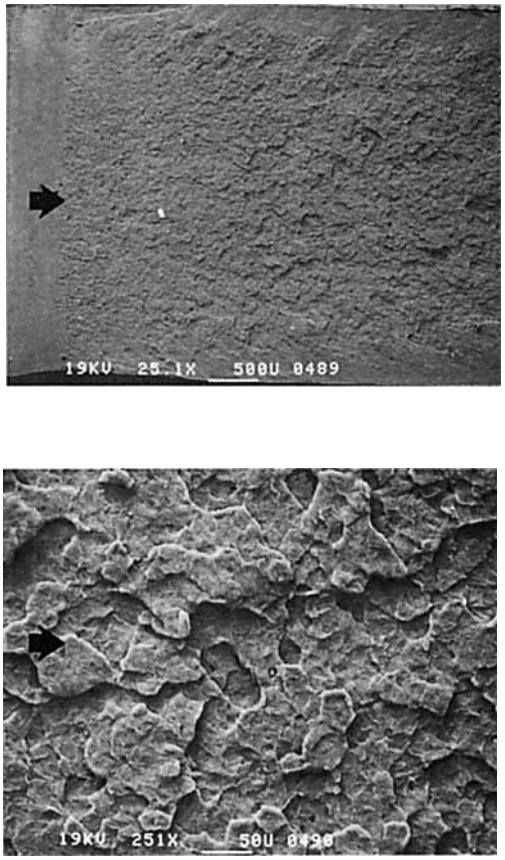

Figure 15 Scanning electron microscopy of nylon 66/Bexloy AP C-803 (90/10) fatigue fracture surface showing patchy-type regions at magnifications of (a) 25× and (b) 250×.

perpendicular to the direction of crack growth. Although fatigue striations were observed in some cases for unmodified nylon 66, the sharp microcracks reported here were not previously noted. It was therefore of interest to carefully examine the transition from a porous patchy texture to the microcracking pattern. Figure 18 demonstrates that the two textures can coexist. Each patch exhibits a unique pattern of microcracks with the orientation of cracking determined by the nucleation and growth of the patchy region. In fact, some of the blends exhibit the microstriations along with the porous texture in the patchy areas even at the initiation of stable fatigue crack propagation.

Figure 19 shows higher magnification views of the microcracking patterns within individual patches. The voids form more densely at the origin of the patchy area with striated microcracking more prevalent as an apparent micropropagation phase of the individual patch. The fan-shaped orientation of the microcracks is clearly unique for each patchy region. Also, a close examination of the microcracking spacing (Fig. 20) indicates that the macroscopic fatigue crack growth rate is a factor of 10 lower than the distance between these surface cracks. It is also possible that the overall crack propagation rate is still dictated by the rate of coalescence of the various patchy regions even though some microcracks may form with each load application. During the latter stages of fatigue crack propagation, when no patchy regions are seen [Fig. 17(b)], the striation spacing is similar to the macroscopically observed crack growth rate (0.005 mm/cycle).

In the case of unmodified nylon 66, the transition from a patchy to a striated morphology was correlated with the temperature increases that occurred due to excessive hysteretic heating at the crack tip.[4] However, it was noted that the heating did not occur at lower frequencies such as 0.5 Hz, which was used

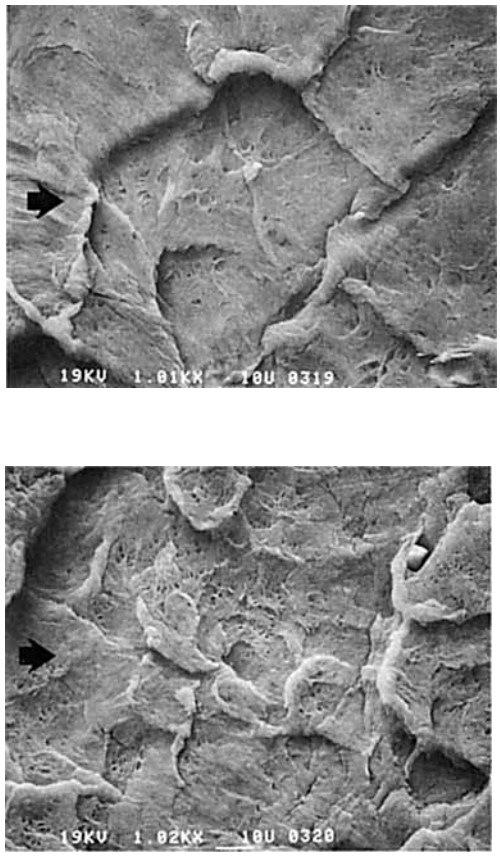

Figure 16 Higher magnification (1000×) views of the fatigue fracture surface of nylon 66 blends showing a porous foamy structure: (a) nylon 66/Bexloy AP C-803 (95/5); (b) nylon 66/Bexloy AP C-803 (90/10).

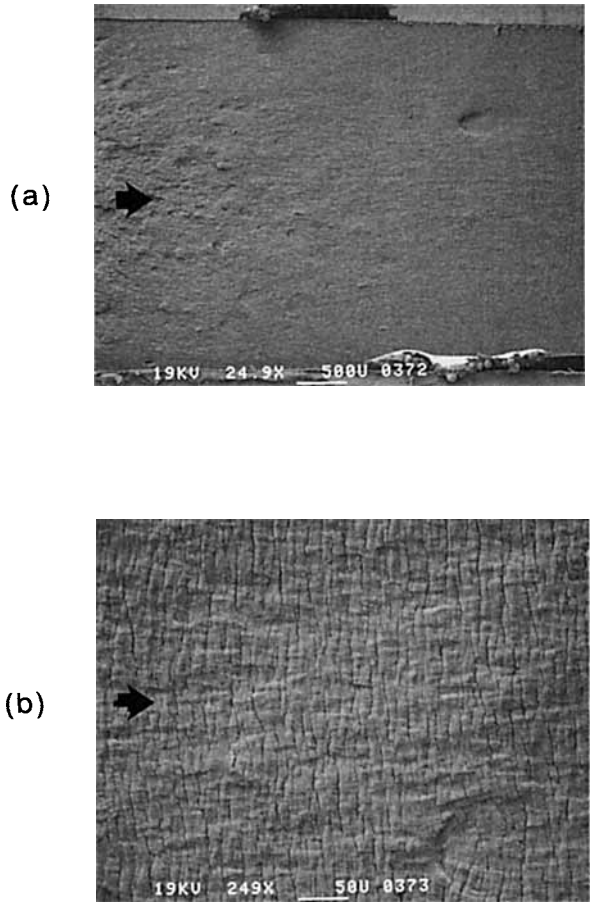

Figure 17 Fatigue fracture surface showing transition from a patchy-type structure to a uniform striated surface for a nylon 66/Bexloy AP C-803 (90/10) blend at (a) 25× and (b) 250×.

in the present study of polymer blends. Thermography studies were therefore carried out for the blended samples. Results indicated that there was no measurable temperature increase during the observed fracture mode transition, i.e., porous patchy to microcracking texture. In fact, in most cases, the crack tip temperature did not exceed 30°C at the end of the fatigue test. It is possible that in some cases temperature increases did occur in the termination stage just prior to rupture of the specimen, but the available results indicate that the deformation transition for the blends and the appearance of striations cannot be attributed to hysteretic heating. Presently, we hypothesize that the change in fracture surface appearance reflects a transition from a mixed mode plane-stress–plane-strain fracture to a more predominantly plane-stress mode as has been reported for acetal fatigue fracture.[13]

DISCUSSION

Compositional Effects

This investigation has demonstrated that fatigue-resistant alloys of nylon 66 can be prepared without employing high concentrations of the alloying polymers. Thus, although fatigue properties are improved, there is no deterioration in the beneficial properties of the crystalline nylon matrix such as modulus or processability. Similarly, it can be anticipated that the good chemical resistance and heat resistance of the matrix will be retained. Although it is not surprising that rubber-toughening agents can retard the propagation of fatigue cracks, the efficiency of relatively low amounts of rubber was unexpected. Furthermore, the beneficial effect of the amorphous nylon has been clearly shown when used in combination with the reactive rubber modifiers.

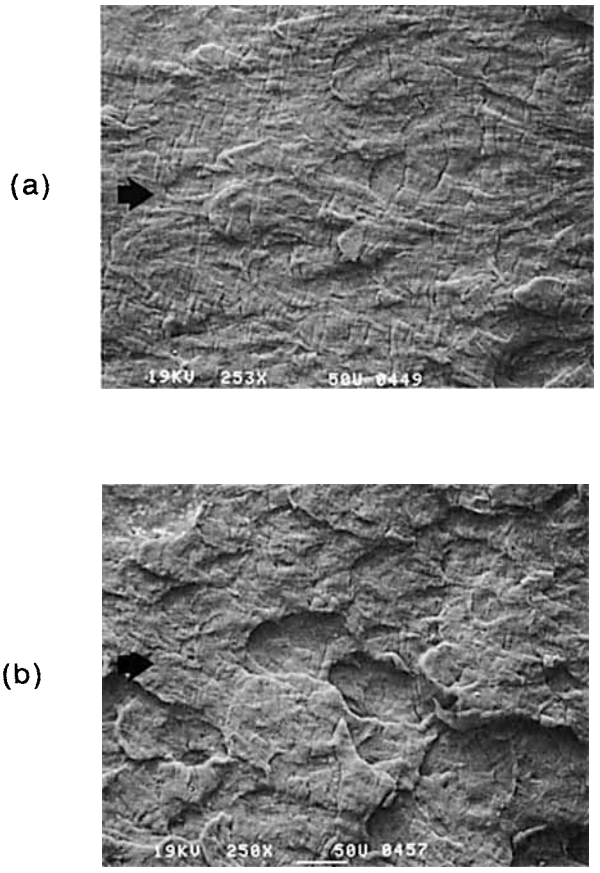

Figure 18 Fatigue fracture surface of nylon 66 blends showing coexisting patchy regions with microcracking: (a) nylon 66/Bexloy AP C-803 (95/5), 250×, and (b) nylon 66/Bexloy AP C-803 (90/10), 250×.

(a)

(b)

Figure 19 Higher magnification views (1000×) of the individual patchy regions showing cavitation and microcracking patterns in a nylon 66/X465 (96/4) blend.

The reason for the improved performance of the ternary blends is not known. It is possible that the miscibility of the amorphous nylon in the nylon 66 matrix allows an improved dispersion of the rubber phase. This is currently being investigated with transmission electron microscopy.

Mechanism for Crack Retardation

The fractography of the blends suggests that the basic fatigue crack propagation by craze coalescence in the nylon 66 matrix, which was reported earlier,[12] is not changed by the addition of alloying ingredients. The size of the patchy regions is not changed by alloying and there is no reason to modify our earlier conclusion that the crazes are nucleated by dust or other foreign particles. In addition, there is no evidence for crack tip blunting in the blends compared to the unmodified nylon 66. What is different for the blends is that the individual patchy regions no longer appear to spontaneously rupture. Thus, the retardation in overall fatigue crack propagation rate is caused in part by a greatly reduced rate of breakdown of the individual crazed regions. In part, this is indicated by the extensive cavitation and associated shear yielding of the matrix and also by the formation of microstriations and/or microcracks within the patches (crazes). Further comment on the mechanism for fatigue crack retardation must await a detailed study of the damage zone and associated deformation processes at the crack tip.

Impact vs. Fatigue Fracture

A correlation between fatigue fracture resistance and fracture toughness has been reported in the literature and a general relationship between fatigue and high rate impact strength had been anticipated.[1] A fracture toughness correlation had been shown for nylon polymers with and without glass fiber rein-

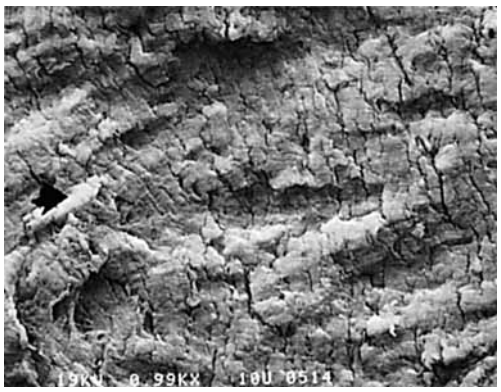

(a)

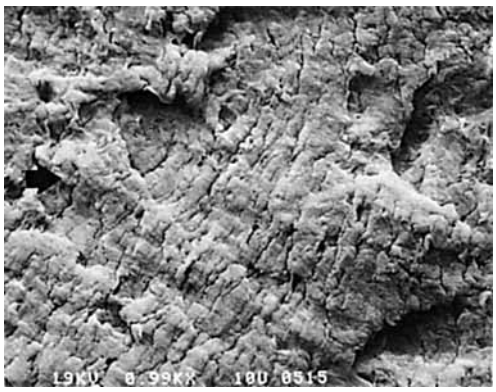

(b)

Figure 20 Higher magnification views (1000×) of the microcracking patterns in a nylon 66/Trogamid T/X465 (90/4/6) blend.

forcement in earlier work.[6] However, for the nylon blends and alloys, it is now apparent that such a simple relationship does not exist. Both the rubber-toughened amorphous nylon and the Noryl GTX exhibit superior impact strength compared to unmodified nylon 66; yet, both of these materials evidenced accelerated fatigue crack growth rates. Similarly, the blends based upon nylon 66 were shown to have greatly improved fatigue resistance while exhibiting little or no improvement in impact strength. All these examples indicate that fatigue fracture and impact fracture involve different mechanisms and one should therefore not expect a general correlation between them. This most likely reflects the time scale of the deformation and corresponding crack speeds. For example, a previous study[4] showed that the fatigue fracture mechanism for unfilled nylon involves a significant contribution from viscoelastic creep.

A similar assessment of the creep contribution was measured for the blends from the frequency dependence of the crack propagation rate data. Essentially no change was noted in the magnitude of the creep contribution for the blends compared to the unmodified nylon 66. Thus, the true fatigue contribution is significantly lower for the blends even in the absence of viscoelastic creep even though the higher rate impact tests show little difference. Besides the crack speed differences between fatigue and impact resistance, this study has also reinforced the general observation that crystalline structure is important for fatigue resistance. It is therefore clear that fatigue-resistant alloys and blends may be quite different in composition from those optimized for impact strength.

The scanning electron microscopy was performed by Curtis Wong of the GM Research Laboratories Analytical Chemistry Department.

REFERENCES

1. R. W. Hertzberg and J. A. Manson, *Fatigue of Engineering Plastics,* Academic Press, New York, 1980.
2. R. W. Lang, J. A. Manson, and R. W. Hertzberg, in *The Role of the Polymeric Matrix in the Processing and Structural Properties of Composite Materials,* J. C. Seferis and L. Nicolais, Eds., Plenum, New York, 1983, p. 377.
3. R. W. Hertzberg, M. D. Skibo, J. A. Manson, and J. K. Donald, *J. Mater. Sci.,* **14,** 1754 (1979).
4. M. G. Wyzgoski, G. E. Novak, and D. L. Simon, *J. Mater. Sci.,* **25,** 4501 (1990).
5. D. C. Martin, G. E. Novak, and M. G. Wyzgoski, *J. Appl. Polym. Sci.,* **37,** 3029 (1989).
6. M. G. Wyzgoski and G. E. Novak, *J. Mater. Sci.,* **26,** 6314 (1991).
7. T. S. Ellis, *Polymer,* **29,** 2015 (1988).
8. S. Y. Hobbs and M. J. E. Dekkers, *J. Mater. Sci.,* **24,** 1316 (1989).
9. H. J. Sue and A. F. Yee, *J. Mater. Sci.,* **24,** 1447 (1989).
10. *1983 Annual Book of ASTM Standards,* American Society for Testing and Materials, Section 3, Vol. 03.01, E647-83, 1983, p. 718.
11. A. Moet and A. Chudnovsky, *J. Mater. Sci.,* **20,** 1934 (1985).
12. M. G. Wyzgoski and G. E. Novak, *Polym. Eng. Sci.,* **32**(16), 1114 (1992).
13. J. Runt and K. P. Gallagher, *J. Mater. Sci.,* **26,** 792 (1991).

Received January 29, 1993
Accepted July 7, 1993